Title

Molecular magnetisabilities computed via finite fields: assessing alternatives to MP2 and revisiting magnetic exaltations in aromatic and antiaromatic species

Journal

Molecular Physics, 119(21-22)

ISSN

0026-8976

Authors

Stauch, Tim
Ganoe, Brad
Wong, Jonathan
et al.

Publication Date

2021-11-17

DOI

10.1080/00268976.2021.1990426

Peer reviewed

Molecular Magnetizabilities Computed Via Finite Fields: Assessing Alternatives to MP2 and Revisiting Magnetic Exaltations in Aromatic and Antiaromatic Species

Tim Stauch,[*1,2,3,4] Brad Ganoe,[*1] Jonathan Wong,[*1]
Joonho Lee,[1] Adam Rettig,[1] Jiashu Liang,[1] Jie Li,[1]
Evgeny Epifanovsky,[5] Teresa Head-Gordon[1,6] and Martin Head-Gordon[1,7]

[1]*Kenneth S. Pitzer Center for Theoretical Chemistry, Department of Chemistry, University of California, Berkeley, California 94720, United States of America*
[2]*Present Address: University of Bremen, Institute for Physical and Theoretical Chemistry, Leobener Straße NW2, D-28359 Bremen, Germany*
[3]*Present Address: Bremen Center for Computational Materials Science, University of Bremen, Am Fallturm 1, D-28359 Bremen, Germany*
[4]*Present Address: MAPEX Center for Materials and Processes, University of Bremen, Bibliothekstraße 1, D-28359 Bremen, Germany*
[5]*Q-Chem Inc., Pleasanton, California 94588, United States of America*
[6]*Department of Chemical and Biomolecular Engineering, University of California, Berkeley, California 94720, United States of America*
[7]*Chemical Sciences Division, Lawrence Berkeley National Laboratory, Berkeley, California 94720, United States of America*

Abstract: Magnetic properties of molecules such as magnetizabilities represent second order derivatives of the energy with respect to external perturbations. To avoid the need for analytic second derivatives and thereby permit evaluation of the performance of methods where they are not available, a new implementation of quantum chemistry calculations in finite applied magnetic fields is reported. This implementation is employed for a collection of small molecules with the aug-cc-pVTZ basis set to assess

[*] = authors contributed equally.
Corresponding author email address: mhg@cchem.berkeley.edu

orbital optimized (OO) MP2 and a recently proposed regularized variant of OOMP2, called κ-OOMP2. κ-OOMP2 performs significantly better than conventional second order Møller-Plesset (MP2) theory, by reducing MP2's exaggeration of electron correlation effects. As a chemical application, we revisit an old aromaticity criterion called magnetizability exaltation. In lieu of empirical tables or increment systems to generate references, we instead use straight chain molecules with the same formal bond structure as the target cyclic planar conjugated molecules. This procedure is found to be useful for qualitative analysis, yielding exaltations that are typically negative for aromatic species and positive for antiaromatic molecules. One interesting species, N_2S_2, shows a positive exaltation despite having aromatic characteristics.

1 Introduction

The magnetizability, $\boldsymbol{\xi}$ of a molecule is the magnetic analog of the electric polarizability. $\boldsymbol{\xi}$ is a second order property that describes the temperature-independent quadratic change of the energy of a molecule, $\delta E(\mathbf{B}) = -\frac{1}{2}\mathbf{B}^{\dagger}\boldsymbol{\xi}\mathbf{B} + \ldots$, in response to the presence of a magnetic induction, $\mathbf{B}$. Thus $\boldsymbol{\xi}$ is a 3×3 matrix (or symmetric rank-2 tensor). For molecules with non-zero total angular momentum (most commonly, unpaired electron spins), there is an additional temperature-dependent contribution that depends directly on the total spin, and, when present, it is typically the largest contribution. $\boldsymbol{\xi}$ also yields the temperature-independent magnetic moment, $\mathbf{m(B)}$ of a molecule induced by $\mathbf{B}$, as $\mathbf{m(B)} = \boldsymbol{\xi}\mathbf{B} + \ldots$. For more background material on magnetostatics and the magnetizability, we refer the reader to several excellent textbooks.[1–3]

The calculation of magnetic properties is based on the pioneering work by Ramsay in the early 1950s.[4–11] Owing to these efforts, the calculation of Nuclear Magnetic Resonance (NMR) chemical shielding tensors and indirect spin-spin coupling tensors (both second order properties) nowadays belongs to the standard repertoire of the computational chemist and complements the experimental interpretation of NMR spectra.[12,13] While magnetizabilities are not amongst the most commonly calculated molecular properties, they have some established roles in chemistry. The main role is molecular magnetism in inorganic chemistry, where unpaired spins and orbital angular momentum are routinely characterized.[14] That is not our focus, so we turn next to applications that do not depend on such contributions. In general, the magnetizability tensor is far more difficult to obtain experimentally than chemical shieldings and spin-spin couplings due to the large experimental error bars,[15] so the need for accurate calculations that serve as benchmarks for the experiments is particularly high. At the level of fundamental molecular properties, the magnetizability tensor connects directly to several spectroscopic observables including the molecular

Zeeman effect, the Cotton-Mouton effect, and the interpretation of microwave spectra.[1–3] Separately, in a broader chemical context, it has long been recognized[16] that the magnetizability of aromatic molecules may be enhanced or "exalted" relative to non-aromatic analogs because of the presence of a closed path (or paths) where electrons may move freely in the aromatic case, versus the absence of such a path in the non-aromatic case. Accordingly, calculations of magnetizability exaltations[17,18] represent perhaps the main chemical application of this molecular property in closed shell, stable molecules. Interestingly, it has also been reported that the level of agreement between mean-field Hartree-Fock magnetizabilities of aromatic molecules and experimentally derived values is significantly poorer for aromatic molecules than for non-aromatic organic molecules.[15]

Magnetizabilities have been calculated fairly early[19,20] and a plethora of electronic structure methods are available for this task: Magnetizabilities at the levels of Hartree-Fock (HF),[15,21] density fitted HF,[22] Density Functional Theory (DFT),[23] Current-Density Functional Theory (CDFT),[24] Magnetic-Field Density Functional Theory (BDFT),[25] the Second-Order Polarization Propagator Approximation (SOPPA),[26] various Coupled-Cluster Polarization Propagator Approximations (CCDPPA, CCSDPPA),[26] Linearized Coupled-Cluster Doubles (L-CCD),[27,28] Coupled-Cluster Singles and Doubles (CCSD),[29] Multiconfigurational Self-Consistent Field (MCSCF),[30,31] Second- and Third-Order Møller-Plesset Perturbation Theory (MP2 and MP3),[27,28,32,33] as well as Resolution-of-the-Identity MP2 (RI-MP2)[34] have been reported. Relativistic effects have been included in the calculation of magnetizabilities at the MP2 level as well.[35]

The "gold-standard" for the calculation of magnetizabilities is CCSD with a perturbative triples correction (CCSD(T))[36] at the complete basis set limit, which has been used to generate the reference data in one of the few benchmark studies for magnetizabilities.[37,38] However, due to the steep scaling of CCSD(T) and the resulting rapid increase of computational cost with increasing system size, such calculations are prohibitive for larger molecules. Hence, more cost-efficient methods for the accurate

calculation of magnetizabilities are desirable.

MP2 is a technique that scales with the fifth power of the number of basis functions ($O(\mathrm{N}^5)$) and has been used successfully in a multitude of applications. While NMR shielding constants calculated with MP2 are typically of satisfying accuracy,[12] the results for magnetizabilities are generally disappointing and often worse than the HF results.[34] This observation has been attributed to the subtle influence of electron correlation on magnetizabilities and the propensity of MP2 to overestimate this effect.

The challenges of MP2 for accurately describing electron correlation have at least two origins. First, it is well-known that HF orbitals yield charge distributions that are too ionic; this limitation can be addressed by optimizing orbitals in the presence of MP2 correlation.[39–42] Second, the form of MP2 correlation means that the total energy is not bounded from below and can become non-variational (i.e. over-correlated) when energy gaps become small. This can be addressed by intelligent denominator regularization schemes (the simplest being just a level shift[43,44]), or, possibly other formalisms.[45] Recently, some of us have presented a new approach to regularized Orbital-Optimized MP2 (κ-OOMP2),[46–48], which scales as the fifth power of the number of basis functions, albeit with a larger prefactor than canonical MP2. κ-OOMP2 attenuates the overestimation of electron correlation by canonical MP2 for small-gaps, while leaving large-gap contributions unaltered. The κ-OOMP2 orbitals have also been used to greatly improve the numerical performance of MP3 relative to HF orbitals.[49] Considering these encouraging results, we think it is useful to explore the performance of κ-OOMP2 for magnetizabilities, particularly given the poor performance of MP2 for this property.

In this paper, the implementation and calculation of magnetizability tensors with κ-OOMP2 is presented using a fully numerical approach. This entails evaluating the energy in the presence of specific applied values of magnetic induction, followed by a finite difference evaluation of the magnetizability. Approaches of this type have been employed previously to characterize the electronic structure of molecules in

nonuniform magnetic fields.[50] To address the gauge origin problem inherent in the calculation of magnetic properties,[12] we use Gauge-Including Atomic Orbitals (GIAOs),[51] also known as London orbitals. Our results demonstrate that the errors of the numerical derivative as compared to the analytical approach are acceptable, and also suggest that κ-OOMP2 performs significantly better for magnetizabilities than standard MP2.

The rest of the paper is structured as follows: After an in-depth discussion of the theoretical background of the calculation of magnetizability tensors with κ-OOMP2 and evaluating the accuracy of the numerical procedure (Section 2), the performance of the new computational method as compared to CCSD(T) reference data, taken from the test set by Lutnæs and co-workers,[37] is assessed (Section 3). After some additional benchmark tests on conjugated cyclic molecules, we then consider a chemical example: magnetizability exaltations, which were historically used to evaluate aromaticity of ring molecules. We present a straightforward approach to evaluating the exaltations without the need for empirical reference data. Conclusions are given in Section 4.

2 Theoretical Background

An in-depth treatment of the quantum chemical calculation of magnetic properties is beyond the scope of this paper. The interested reader is kindly referred to existing reviews on the subject.[12,13,52] Instead, here the general design idea of our code (Section 2.1), the matrix elements that are required for the calculation of magnetizabilities (Section 2.2), the particularities of κ-OOMP2 in the calculation of the magnetizability tensor (Section 2.3), details on the implementation and verification of our code (Section 2.4) as well as the performance of the numerical implementation compared to analytical results (Section 2.5) are discussed.

2.1 General Approach

The magnetizability $\boldsymbol{\xi}$ is a 3x3 tensor and can be calculated as the second derivative of the energy E w.r.t. the magnetic field $\mathbf{B}$,[12] with elements

$$\xi_{ij} = -\frac{\mathrm{d}^2 E\left(\{\mathbf{R}_N\}, \mathbf{B}\right)}{\mathrm{d}B_i \mathrm{d}B_j}\bigg|_{\mathbf{B}=\mathbf{0}} \quad . \tag{1}$$

Here, $\{\mathbf{R}_N\}$ is the nuclear configuration. The isotropic magnetizability is $\xi_{\text{iso}} = \frac{1}{3}\text{tr}(\boldsymbol{\xi})$. We use Gauge-Including Atomic Orbitals (GIAOs),[51] also known as London orbitals, in the calculation of magnetizabilities to address the gauge-origin problem.[12] A GIAO ω_μ, centered on nucleus N, is given as

$$\omega_\mu(\mathbf{r}; \mathbf{A}_N) = \exp\left(-i\mathbf{A}_N \cdot \mathbf{r}\right) \cdot \chi(\mathbf{r}), \tag{2}$$

where $\mathbf{r}$ is the electron coordinate and $\chi(\mathbf{r})$ is a regular Gaussian-type orbital and the vector potential $\mathbf{A}_N$ is

$$\mathbf{A}_N = \frac{1}{2}\mathbf{B} \times \mathbf{R}_{NO}. \tag{3}$$

$\mathbf{R}_{NO}$ is the vector from the nucleus N to an arbitrarily chosen gauge-origin O, the latter of which we choose to be the zero vector for convenience.

We use a fully numerical implementation for the calculation of the magnetizability tensor (eq. 1). In particular, focusing on the isotropic part of the magnetizability tensor and omitting the electronic and nuclear coordinates in the energy for clarity, we calculate the second derivative of the energy w.r.t. the magnetic field to second order *via*[53]

$$\xi_{ii} = -2\frac{E(\Delta B_i) - E(\mathbf{B} = \mathbf{0})}{\Delta B_i^2} \tag{4}$$

Off-diagonal elements of the tensor can be evaluated to second order via the following expression:

$$\xi_{ij} = -\frac{E(\Delta B_i) + E(-\Delta B_i) + E(\Delta B_j) + E(-\Delta B_j) - 4E(\mathbf{B} = \mathbf{0})}{2\Delta B_i \Delta B_j} \tag{5}$$

There are also corresponding expressions that are accurate to fourth order,*via*[53] which is as follows for the diagonal elements:

$$\xi_{ii} = -\frac{-\frac{1}{6}E(2\Delta B_i) + \frac{8}{3}E(\Delta B_i) - \frac{5}{2}E(\mathbf{B} = \mathbf{0})}{\Delta B_i^2}, \tag{6}$$

ΔB_i is the step in the Cartesian component i of the magnetic field. The choice of this parameter determines the accuracy of the numerical results. An assessment of ΔB_i and its relation to the numerical error is given in Section 2.5. The calculation of the magnetizability *via* eqs. 4 and 6 necessitates the calculation of several energies at different values of the magnetic field, which has been achieved before.[54,55] Due to the use of GIAOs, we use a fully complex-valued code throughout our calculations.

Although analytical derivatives are generally to be preferred over their numerical counterparts due to some clear advantages (e.g. typically shorter calculation times, significantly reduced numerical noise, real-valued code, and no need to calibrate/validate a choice of the finite difference step size), we chose a fully numerical scheme here to calculate the magnetizability for the following reasons: Firstly, once the energy expressions in an external magnetic field (cf. Section 2.2) are implemented, it is fairly straightforward to add and rapidly test new computational methods for the calculation of magnetic properties, since the cumbersome implementation of the analytical expressions, which needs to be carried out for each level of theory separately, is avoided. Secondly, the implementation of the explicit energy expressions in the presence of an external magnetic field allows the rapid adaption to other properties involving the magnetic field (e.g. chemical shieldings, circular dichroism), since only a handful of new terms needs

to be implemented. This is much more cumbersome in the case of analytical calculations. Thirdly, the calculation of magnetic properties like chemical shieldings or spin-spin couplings for only specific nuclei or pairs of nuclei, respectively, can be trivially achieved with numerical derivatives, although analytical calculations of magnetic properties of subsets of atoms have been reported.[56] Finally, parallelization of the code is a trivial task, since the calculations of the perturbed energies can be conducted independently on different computer nodes, with no need of communication between the processors. This is especially valuable considering today's highly parallel computer infrastructure. In principle, given enough processors, the calculation of the magnetizability is roughly as computationally costly as the calculation of an energy in the presence of a finite magnetic field. Hence, in order to test the viability of the κ-OOMP2 method for the calculation of magnetizabilities, we chose a fully numerical approach.

2.2 Required Matrix Elements

The Hamiltonian in an external magnetic field is discussed in detail in ref. 57 and an excellent overview on the calculation of matrix elements involving GIAOs can be found in ref. 58. For the sake of brevity, we will in the following only discuss those matrix elements that we have implemented for the calculation of magnetizabilities.

Focusing on the one-electron terms first, the kinetic energy matrix elements are defined as

$$h_{\mu\nu}^{\text{kin}} = \left\langle \omega_\mu \middle| -\frac{1}{2}\nabla^2 \middle| \omega_\nu \right\rangle . \tag{7}$$

Using well-known relations,[59] eq. 7 can be reduced to linear combinations of overlap integrals $\langle \omega_\mu | \omega_\nu \rangle$ between GIAOs.

One-electron matrix elements associated with electron-nuclear attraction (NA) are defined as

$$h_{\mu\nu}^{\mathrm{NA}} = -\left\langle \omega_\mu \middle| \sum_\alpha \frac{Z_\alpha}{r_\alpha} \middle| \omega_\nu \right\rangle , \tag{8}$$

where r_α is the distance between the electron and the nucleus α. The calculation of such matrix elements requires the use of the Boys function with a complex argument. The interested reader is referred to ref. 58 for details.

For the calculation of the magnetizability tensor, two more one-electron terms need to be taken into account. The first one involves the diamagnetic magnetizability (DM) operator,[57]

$$\hat{h}^{\mathrm{DM}} = \frac{1}{8}\left[\mathbf{B}^2 \cdot \mathbf{r}^2 - (\mathbf{B}\cdot\mathbf{r})^2\right] . \tag{9}$$

The second one involves the paramagnetic shielding (PS) operator,

$$\hat{h}^{\mathrm{PS}} = -\frac{i}{2}\mathbf{B}\cdot(\mathbf{r}\times\nabla) . \tag{10}$$

After some straightforward yet somewhat cumbersome algebra, both operators lead to energy expressions that involve only overlap integrals with increased or decreased angular momentum on GIAO ω_ν (see Appendix).

Turning to the two-electron integrals, many schemes for the calculation of the crucial electron repulsion are available. Some of the most prominent ones are known as Taketa-Huzinaga-O-ohata (THO66),[60] McMurchie-Davidson,[61] Rys-quadrature,[62,63] Gill-Johnson-Pople (GJP),[64] and Head-Gordon-Pople (HGP88).[65] For an efficient calculation of the electron repulsion integrals it is well-known that the optimal choice of algorithm depends on the orbital angular momentum.[58] Initially, we implemented the

inefficient but rather straightforward THO66 algorithm to generate reference numbers (cf. Section 2.4), but later switched to the much more efficient HGP88 algorithm for production calculations for both 2-electron-4-center integrals for the regular electron repulsion and 2-electron-3-center integrals for the Resolution-of-the-Identity approximation (for which efficient evaluation has recently been described[66]). All values reported in this paper have been generated with the HGP88 algorithm.

Hence, we have only implemented three basic types of integrals, i.e. overlap, nuclear attraction and electron repulsion. All other integrals (kinetic energy, diamagnetic magnetizability and paramagnetic shielding) could be reduced to linear combinations of overlap integrals.

2.3 Magnetizabilities with κ-OOMP2

The regularized orbital-optimized MP2 approach (κ-OOMP2) has been presented recently by some of us.[46–48] In the following only a brief overview of the approach that is necessary to understand the gist of the method is given. The interested reader is kindly referred to the original publication for details.

In canonical MP2, the Hylleraas functional L is minimized with respect to the amplitudes t, which yields the MP2 energy,

$$E_{\text{MP2}} = \min_t L[t, \theta]. \tag{11}$$

where the Hylleraas functional is

$$L[t, \theta] = \langle \Psi_1 \big| \hat{H} \big| \Psi_0 \rangle + \langle \Psi_0 \big| \hat{H} \big| \Psi_1 \rangle + \langle \Psi_1 \big| \hat{H}_0 - E_0 \big| \Psi_1 \rangle \tag{12}$$

In OOMP2, the Hylleraas functional is furthermore optimized with respect to orbital rotation parameters θ,

$$\frac{\partial L[t,\theta]}{\partial \theta} = 0 \tag{13}$$

This approach yields a set of orbitals that are no longer the Hartree-Fock orbitals, but approximations to Brueckner orbitals.[39,67–69] As GIAOs are used in the calculation of magnetic properties, the resulting orbitals are still gauge-including. Hence, the results are independent of the (arbitrary) choice of gauge origin. OOMP2 scales as $O(\mathrm{N}^5)$, albeit with a larger prefactor than canonical MP2, due to the requirement to optimize the orbitals iteratively.

In κ-OOMP2, one modifies the Hylleraas functional by damping the two-electron integrals via $\langle ab||ij\rangle \longleftarrow \langle ab||ij\rangle \left(1 - \exp\left(-\kappa\Delta_{ij}^{ab}\right)\right)$ such that the MP2 amplitudes t are modified as

$$t_{ij}^{ab} = \frac{\langle ab||ij\rangle}{\Delta_{ij}^{ab}} \left(1 - \exp\left(-\kappa\Delta_{ij}^{ab}\right)\right), \tag{14}$$

Here $\Delta_{ij}^{ab} = \epsilon_a + \epsilon_b - \epsilon_i - \epsilon_j$ in terms of orbital energies, ϵ, of virtual levels, a, b and occupied levels, i, j. These regularized amplitudes lead to the regularized MP2 (κ-MP2) energy expression

$$E_{\kappa\text{-MP2}} = -\frac{1}{4}\sum_{ijab} \frac{|\langle ab||ij\rangle|^2}{\Delta_{ij}^{ab}} \left(1 - \exp\left(-\kappa\Delta_{ij}^{ab}\right)\right)^2, \tag{15}$$

If $\Delta_{ij}^{ab} \to 0$, $t_{ij}^{ab} \to \kappa \langle ab||ij\rangle$ instead of ∞, and the corresponding correlation energy contribution tends to zero. This has the obvious advantage that systems with near-degenerate energy levels can be treated, which is problematic with unregularized MP2.[46] The removal of divergence can, in fact, be achieved by a rather simple linear shift as well.[43,44] The particular form in Eq. 14 was chosen not only to regularize the offending energy denominator but also to maintain the well-behaved correlation energy contribution coming from large denominators. When combined with orbital optimization, such an energy-dependent

regularizer was found to be essential to outperform unregularized MP2 and OOMP2 over a handful of benchmark sets while restoring the Coulson-Fischer point.[46,49] Since κ-OOMP2 has displayed a propensity of attenuating the overestimation of electron correlation that canonical MP2 exhibits, κ-OOMP2 is a promising approach to improve the performance of MP2 in the calculation of magnetizability tensors.

Our κ-OOMP2 code uses the resolution-of-the-identity (RI) approximation throughout.[46] In this approach, the fitting basis is a regular Gaussian-type basis and not a GIAO basis, because otherwise the crucial requirement of gauge-independence cannot be met.[22] The Resolution-of-the-Identity approximation has been used before in combination with MP2 for the calculation of NMR shielding tensors[22,70] and magnetizabilities.[34] The errors of the RI approximation have been shown to be negligible throughout. The energy before the first orbital-optimization cycle is the RI-MP2 energy, which allows us to calculate magnetizabilities at the RI-MP2 level of theory as well.

2.4 Implementation and Code Verification

We have implemented all one- and two-electron integrals given in Section 2.2 and κ-OOMP2 using GIAOs in the integral library `libqints` in a developer's version of Q-Chem 5[71,72] Our code is able to run complex-restricted[48,73] and complex-general[47,74] SCF procedures as implemented in `libgscf` and `libgmbpt`, the latter of which is important for the calculation of indirect spin-spin coupling constants (to be presented in a future publication).

In a first step, the matrix elements were tested in order to verify our code. The overlap matrix elements were tested against reference results obtained *via* Mathematica.[75] The Mathematica code for the overlap integrals was taken from ref. 76 and adapted for GIAOs. Although the kinetic energy integrals can be decomposed to the already verified overlap integrals, the former were tested separately against Mathematica references[77] that were again adjusted for GIAOs. A similar procedure was carried out for nuclear attraction

integrals, for which numerical Mathematica references[78] with GIAOs were generated. The diamagnetic magnetizability and the paramagnetic shielding integrals, which are needed in the calculation of the magnetizability tensor, were also implemented in Mathematica to verify our implementation of the relations given in the Appendix. To test the electron repulsion integrals, we implemented both the THO66[60] and the HGP88[65] algorithms in Q-Chem, both for 2-electron-4-center and 2-electron-3-center integrals. Both codes give matching values for any applied magnetic field.

As another (weak) test of the implementation we verified that the overlap, nuclear attraction, kinetic energy and electron repulsion integrals reduce to the results of regular Gaussian type orbitals at zero magnetic field. In the case of the diamagnetic magnetizability and paramagnetic shielding integrals the results are trivially zero if no magnetic field is applied.

In the second verification step, magnetizabilities at the Hartree-Fock level were tested against the Dalton program package.[79] Magnetizabilities at the RI-MP2 level with very large auxiliary basis sets were tested against MP2 results obtained *via* CFOUR.[80] CFOUR was also employed to generate CCSD and CCSD(T) results against which the various MP2 methods can be assessed.

In the third verification step, magnetizabilities at the κ-OOMP2 level were tested at its two limits: $\kappa = 0$ against those at the Hartree-Fock level and $\kappa = \infty$ against those at the OOMP2 level.

2.5 Numerical Accuracy of Finite Differences Magnetizability

To evaluate the numerical accuracy of the finite difference scheme, we tested the finite difference HF and RI-MP2 magnetizabilities of various small molecules against analytical HF and MP2 magnetizabilities obtained via CFOUR. The general issue in choosing an acceptable step size is avoiding numerical noise from limited precision in the energy (step size not too small) whilst also avoiding contamination from higher derivatives in the target second order property (step size not too big). We chose C_2H_4 as an example

of molecules with small HOMO-LUMO gaps that might be prone to contamination from higher order terms with larger step sizes; H_4C_2O as the largest molecule in the test set that should accentuate numerical error with smaller step sizes; and lastly LiH as an in-between molecule with moderate gap and small size. The cc-pVDZ, aug-cc-pVDZ, and cc-pVTZ basis sets were tested in this manner. The SCF convergence criteria was 10^{-11} a.u., and the cutoff threshold for two electron integrals was 10^{-14} a.u.

In Table 1 we present the % error for HF magnetizabilities for the three aforementioned molecules. With the second order finite difference scheme, the optimal step size 10^{-3} a.u. for C_2H_4 and H_4C_2O leads to errors on the order of $10^{-4}\%$ or less for all three basis sets tested; whereas the optimal step size 10^{-4} a.u. for LiH leads to % errors on the order of $10^{-5}\%$ for the cc-pVDZ and cc-pVTZ basis sets, and we observe a shift in aug-cc-pVDZ: the optimal step size 10^{-5} a.u. leads to % error on the order of $10^{-4}\%$. Overall these results are encouraging because a step size of either 10^{-3} or 10^{-4} is acceptable for all three molecules in all three basis sets.

The assessment of the numerical accuracy of our finite difference RI-MP2 implementation of the magnetizability is more complicated, since the RI approximation constitutes an additional error source (CFOUR is using exact integrals). To disentangle the RI error from the error of the numerical procedure, we tested two different auxiliary basis sets (rimp2-cc-pVDZ and rimp2-aug-cc-pVTZ) for the C_2H_4 and H_4C_2O molecules (Tables 2 and 3). The smaller rimp2-cc-pVDZ basis reveals error limits associated with the RI approximation. With the larger aug-cc-pVDZ and cc-pVTZ basis sets, applying the rimp2-aug-cc-pVTZ auxiliary basis leads to at least an order of magnitude of error improvement. For all three AO basis sets, using rimp2-aug-cc-pVTZ and either 2^{nd} or 4^{th} order finite difference, at least two orders of magnitude in the B field can be identified that deliver errors better than $10^{-2}\%$. Encouragingly, the optimal range of fields does not appear to depend strongly on the AO basis set for the choices we will use in this work.

Table 1: Numerical performance of the 2nd order finite difference scheme for the magnetizability of three molecules with varying step size. Values shown as percentage error for Hartree-Fock in 3 basis sets. Reference values were calculated analytically at the same level of theory.

Molecule	B field step size (log_{10} a.u.)						
	-6	-5	-4	-3	-2	-1	0
				cc-pVDZ			
C_2H_4	-16.17	-0.0215	0.0015	0.0001	0.0102	0.8680	-40.29
H_4C_2O	21.94	-0.0671	-0.0002	-0.0001	-0.0147	-2.4506	-6.89
LiH	0.2805	0.0037	0.00003	-0.0001	-0.0110	-1.0189	-11.6254
				aug-cc-pVDZ			
C_2H_4	-0.0910	-0.1765	0.0027	-0.00002	-0.0011	0.3695	-44.6909
H_4C_2O	-20.8518	-0.1618	-0.0002	-0.0002	-0.0232	-1.7756	-75.7206
LiH	-3.0791	0.0002	0.0048	0.0043	-0.0342	-3.1063	-1.3800
				cc-pVTZ			
C_2H_4	-5.5078	-0.1462	0.0017	0.0001	0.0084	0.7034	9.7808
H_4C_2O	16.0834	0.0573	-0.0005	-0.0002	-0.0158	-1.6033	-3.1721
LiH	-3.0657	0.0127	-0.00004	-0.0003	-0.0363	-3.2028	1.8863

Overall we recommend using the step size of 10^{-3} a.u. and the 2nd order finite difference scheme, since this combination delivers a satisfying compromise between accuracy and computational cost throughout. Perhaps surprisingly, the relatively small rimp2-cc-pVDZ auxiliary basis set when paired with either of the three AO basis sets (cc-pVDZ, aug-cc-pVDZ, cc-pVTZ) appears to be accurate enough for most applications from a numerical point of view. In our applications below we will nevertheless always use the auxiliary basis set that corresponds to the chosen AO basis.

Table 2: Numerical performance of the finite difference scheme of 2nd or 4th order (FD order) for the magnetizability of C_2H_4 with varying step size. Values shown are percentage errors (%) of RI-MP2 with three AO basis sets (cc-pVDZ, aug-cc-pVDZ, and cc-pVTZ), using two different auxiliary basis sets (rimp2-cc-pVDZ and rimp2-aug-cc-pVTZ) for each one. Reference values were calculated analytically at the MP2 level of theory with the respective basis sets.

Auxiliary basis set	FD order	B field step size (log_{10} a.u.)						
		-6	-5	-4	-3	-2	-1	0
				cc-pVDZ				
rimp2-cc-pVDZ	2	-12.60	-0.0923	-0.0516	-0.0520	-0.0398	1.0116	-38.98
	4	15.75	-0.0837	-0.0464	-0.0521	-0.0521	0.4620	-35.74
rimp2-aug-cc-pVTZ	2	0.9320	-0.3822	-0.0040	-0.0006	-0.0116	1.0567	-40.30
	4	5.871	0.3780	-0.0016	-0.0007	-0.0006	0.5108	-35.16
				aug-cc-pVDZ				
rimp2-cc-pVDZ	2	29.35	-0.3405	-0.0835	-0.0825	-0.0830	0.5057	-43.59
	4	30.39	-0.4837	-0.0804	-0.0825	-0.0839	0.1920	-22.78
rimp2-aug-cc-pVTZ	2	21.46	0.5108	-0.00004	-0.0017	-0.0027	0.5677	-18.82
	4	220.16	0.0478	-0.0029	-0.0017	-0.0031	0.2606	-163.75
				cc-pVTZ				
rimp2-cc-pVDZ	2	50.08	-0.4886	-0.1200	-0.1186	-0.1080	0.8054	16.90
	4	-54.40	-0.4137	-0.1140	-0.1188	-0.1186	0.3506	44.95
rimp2-aug-cc-pVTZ	2	46.44	-0.1503	-0.0066	-0.0060	0.0044	0.9000	1.91
	4	-42.84	0.0659	-0.0080	-0.0061	-0.0061	0.4562	0.20

3 Results and Discussion

3.1 Accuracy of κ-OOMP2 Magnetizabilities for the Lutnæs Set

As a first assessment, we utilized the test set of 28 molecules curated by Lutnæs et al.[37] to assess the accuracy of κ-OOMP2 for isotropic magnetizabilities. In Table 4 we present various statistics for Hartree-Fock (HF), RI-MP2, OOMP2, and κ-OOMP2 in comparison to CCSD(T) in the aug-cc-pVTZ basis. When calculating the RMSE, MSE and the maximum error for each method, we exclude O_3, which exhibits by far the largest correlation effects because of its multireference character. This procedure is in accordance with previous benchmarking studies.[37,38]

In terms of magnitudes, mean-field HF theory performs quite well, with nearly zero mean signed error

Table 3: Numerical performance of the finite difference scheme of 2nd or 4th order (FD order) for the magnetizability of H_4C_2O with varying step size. Values shown are percentage errors (%) of RI-MP2 with three AO basis sets (cc-pVDZ, aug-cc-pVDZ, and cc-pVTZ), using two different auxiliary basis sets (rimp2-cc-pVDZ and rimp2-aug-cc-pVTZ) for each one. Reference values were calculated analytically at the MP2 level of theory with the respective basis sets.

Auxiliary basis set	FD order	B field step size (log_{10} a.u.)						
		-6	-5	-4	-3	-2	-1	0
				cc-pVDZ				
rimp2-cc-pVDZ	2	22.69	-0.0868	-0.0242	-0.0241	-0.0372	-1.4077	-7.84
	4	6.87	-0.0202	-0.0214	-0.0240	-0.0240	0.1199	-27.83
rimp2-aug-cc-pVTZ	2	-40.04	0.0881	-0.0027	-0.0007	-0.0139	-1.3868	-25.89
	4	12.98	0.2546	-0.0001	-0.0006	-0.0006	0.1421	39.07
				aug-cc-pVDZ				
rimp2-cc-pVDZ	2	27.00	0.0308	-0.0343	-0.0300	-0.0512	-1.7195	-73.74
	4	264.99	0.3917	-0.0284	-0.0299	-0.0306	-0.0700	12.35
rimp2-aug-cc-pVTZ	2	56.31	-0.3953	0.0015	-0.0013	-0.0227	-1.6985	-72.59
	4	304.88	0.4405	-0.0089	-0.0012	-0.0020	-0.0467	76.66
				cc-pVTZ				
rimp2-cc-pVDZ	2	17.16	0.0794	-0.0136	-0.0136	-0.0280	-1.5149	-5.61
	4	8.27	-0.1538	-0.0121	-0.0134	-0.0134	0.0875	-16.71
rimp2-aug-cc-pVTZ	2	-2.55	-0.0372	-0.0013	-0.0018	-0.0162	-1.5077	0.50
	4	8.55	-0.1455	-0.0025	-0.0017	-0.0016	0.0974	-2.83

(MSE), indicating no systematic over or under-estimation. Comparing HF with CCSD(T), it is evident that correlation effects are relatively small, on the order of a few percent (with the conspicuous exception of ozone). The performance of MP2, as noted previously,[34] is disappointing. The MSE increases by a factor of 5 relative to HF, and the RMS error is reduced by only 28 %. Ten cases show significant overcorrection, and disturbingly, there are four cases where MP2 corrects in the wrong direction.

Orbital optimization with MP2 significantly improves the results for magnetizabilities. Whilst OOMP2 is a method that typically exaggerates electron correlation effects,[43,46] OOMP2 magnetizabilities nevertheless show improvements in both MSE and RMSE relative to MP2 itself. κ-OOMP2 reduces over-correlation effects in OOMP2 via the use of energy-dependent regularization (Eq. 15). As seen in Table 4, using the recommended parameter[46] ($\kappa = 1.45$) provides significant further improvement relative to OOMP2. At

Table 4: Results and statistics for HF, RI-MP2, OOMP2 and κ-OOMP2 calculations of magnetizability compared to the CCSD(T) reference with the aug-cc-pVTZ basis set, for the Lutnæs data set[37] (10^{-30} JT^{-2}). Note that ozone is excluded from the statistics, because it is a dramatic outlier for HF and MP2.

Molecule	HF	MP2	κ-MP2	OOMP2	κ-OOMP2	CCSD(T)
AlF	-401.02	-406.01	-403.43	-407.81	-404.59	-400.20
C_2H_4	-355.07	-350.16	-348.32	-349.59	-348.29	-345.94
C_3H_4	-478.33	-487.29	-484.23	-485.92	-483.39	-481.68
CH_2O	-139.72	-131.80	-135.15	-128.04	-132.96	-129.14
CH_3F	-318.60	-318.31	-318.19	-316.57	-316.94	-317.36
CH_4	-314.11	-322.03	-319.68	-322.17	-319.66	-318.40
CO	-204.95	-218.34	-215.40	-218.07	-215.12	-213.48
FCCH	-452.94	-448.91	-448.26	-448.53	-448.25	-446.61
FCN	-378.65	-376.50	-376.84	-376.11	-376.78	-374.17
H_2C_2O	-433.22	-440.90	-440.05	-440.17	-439.74	-430.82
H_2O	-231.45	-238.75	-237.05	-239.57	-237.43	-236.21
H_2S	-456.51	-468.40	-463.05	-467.91	-462.61	-461.97
H_4C_2O	-545.26	-542.17	-541.97	-538.21	-539.36	-536.25
HCN	-280.51	-278.44	-277.31	-277.32	-276.86	-275.30
HCP	-512.49	-505.57	-500.33	-504.54	-500.73	-498.39
HF	-172.89	-178.76	-177.97	-179.51	-178.48	-177.43
HFCO	-312.12	-315.12	-315.43	-315.78	-315.85	-310.64
HOF	-244.91	-242.51	-244.11	-238.35	-241.43	-237.34
LiF	-191.32	-198.57	-197.02	-199.71	-197.6	-197.01
LiH	-125.72	-127.04	-122.59	-127.22	-122.71	-129.30
N_2	-203.10	-210.57	-208.46	-209.82	-207.93	-206.15
N_2O	-343.15	-345.39	-345.64	-342.05	-344.05	-340.67
NH_3	-287.56	-294.80	-292.39	-295.23	-292.46	-291.19
O_3	581.49	-637.00	-360.72	-34.59	73.76	112.39
OCS	-598.87	-597.22	-597.26	-592.65	-595.38	-591.09
OF_2	-271.88	-252.39	-258.43	-237.10	-250.43	-249.58
PN	-302.34	-333.65	-324.46	-324.05	-319.92	-314.90
SO_2	-304.00	-336.73	-334.44	-339.45	-334.6	-324.38
RMSE	8.63	6.22	4.93	4.92	3.89	
MSE	-0.93	-4.84	-3.40	-3.18	-2.52	
MaxE	22.30	18.75	10.01	15.07	10.22	

the κ-OOMP2 level, the maximum and RMS errors are both reduced by more than a factor of 2 relative to HF. Relative to MP2 the main improvement is in the ten cases that showed significant overcorrection; the four cases that MP2 corrects in the wrong direction remain.

Finally, it is useful to assess the role of regularization using the unmodified HF orbitals (i.e. the κ-MP2 column of Table 4, again using $\kappa = 1.45$). The improvement of κ-MP2 relative to MP2 is on par with the improvement of κ-OOMP2 relative to OOMP2. At $\kappa = 1.45$, κ-MP2 has similar RMSE and slightly larger MSE than OOMP2, while the max error is significantly reduced, even more so than for κ-OOMP2. Of course κ-MP2 has the benefit of shedding the iterative cost of OOMP2, but it is interesting that the improvements from regularization (κ-MP2) and orbital optimization (OOMP2) are synergistic: κ-OOMP2 is clearly the best-performer of the 4 MP2-based approaches.

It is encouraging that κ-OOMP2 significantly improves upon MP2 for magnetizabilities using the regularization parameter ($\kappa = 1.45$) chosen without reference to this property. To explore the extent to which further improvement is possible, Figure 1 displays how the κ-OOMP2 errors on this 27-molecule dataset vary as a function of κ. Note that $\kappa = 0$ (left edge) is HF, and $\kappa \to \infty$ is OOMP2, so strong regularization is to the left of the figure, whilst weak is to the right. It is evident that modest improvements in magnetizabilities beyond the $\kappa = 1.45$ results are obtained by decreasing κ to about 1.2, which corresponds to somewhat stronger damping of electron correlation effects. However, the κ dependence is sufficiently weak that we recommend using the existing parameter. κ-MP2 has qualitatively similar behaviour as κ-OOMP2, but with slightly worse performance for all 3 statistical measures.

3.2 Accuracy of κ-OOMP2 Magnetizabilities for Conjugated Cyclic Molecules

As one additional assessment of the performance of this set of quantum chemical methods, we revisit the magnetizability anisotropies of a set of aromatic molecules that were previously examined at the HF

Figure 1: Variation of the κ value in κ-MP2 and κ-OOMP2 and its effect on performance on the 27-molecule test set

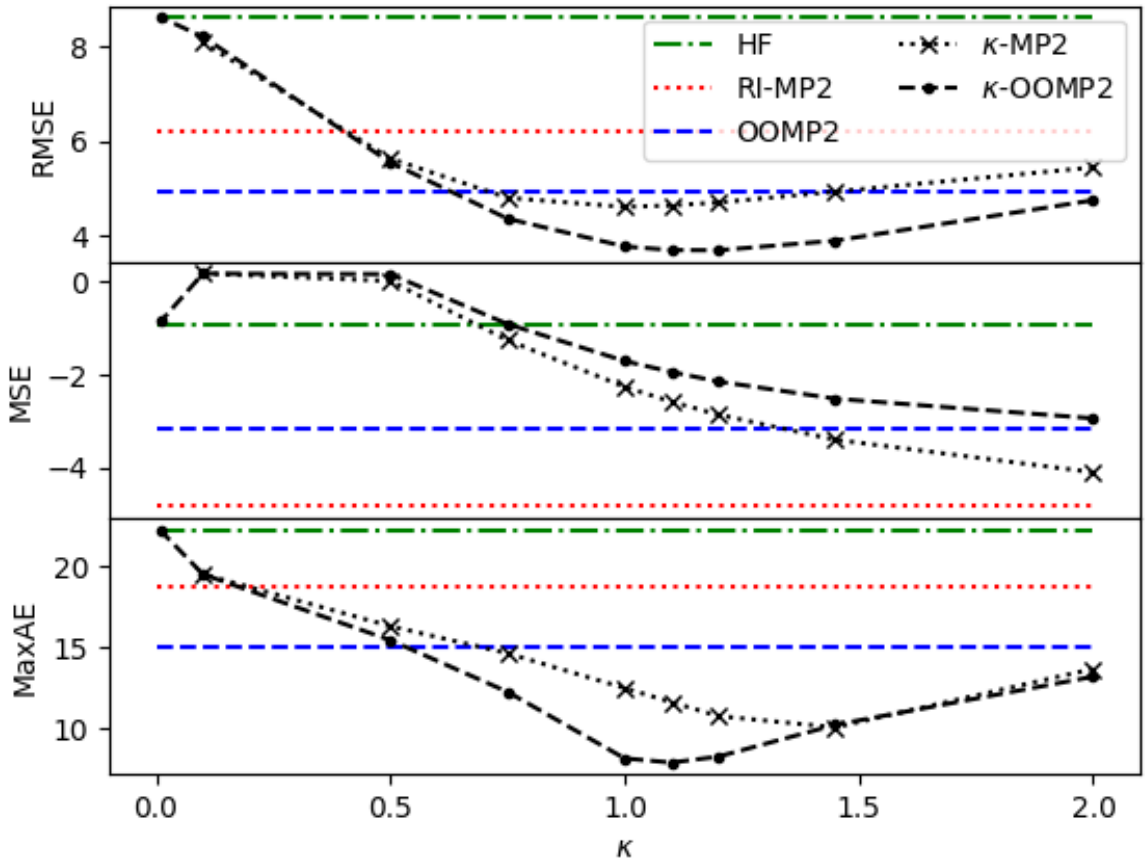

level.[15] These species exhibit greater electron delocalization than the small molecules discussed above, and therefore have larger magnetizabilities. For planar molecules (in the xy plane), the magnetizability anisotropy is defined as

$$\xi_{\text{aniso}} = \xi_{zz} - \frac{1}{2}\left(\xi_{xx} + \xi_{yy}\right) \tag{16}$$

As shown in Table 5, HF anisotropies with the relatively small aug-cc-pVDZ basis set perform quite well relative to experiment, presumably due to fortuitous cancellation between basis set incompleteness effects and neglect of electron correlation. Nevertheless, at least for aromatic species like these, the

aug-cc-pVDZ basis set appears to be quite useful for calculations at the HF level. Basis set incompleteness effects are clearly evident by comparing HF against CCSD(T) relative to experiment: the HF result agrees better in 4 of the 6 cases.

Table 5: Calculated magnetizability anisotropies for various conjugated molecules using the aug-cc-pVDZ basis, and and experimental values (10^{-30} JT^{-2}). Deviations are evaluated with respect to the CCSD(T) results.

Molecule	HF	MP2	OOMP2	κ-OOMP2	CCSD	CCSD(T)	exp.
benzene	-1061.26	-939.85	-922.15	-951.55	-905.92	-878.79	-1036$\pm$40[81]
pyridine	-1079.05	-1033.0	-1007.04	-1037.1	-1012.67	-993.19	-953$\pm$12[82]
furan	-644.59	-702.74	-702.31	-691.76	-654.65	-660.30	-643$\pm$8[83]
thiophene	-854.57	-927.42	-930.06	-907.08	-863.56	-871.27	-832$\pm$18[83]
1,3-dioxol-2-one	-242.01	-253.65	-249.35	-250.39	-241.54	-244.136	-240$\pm$20[20]
cyclopentadiene	-558.40	-601.50	-609.76	-593.32	-554.20	-561.91	-570$\pm$5[20]
RMSE	82.88	44.58	40.02	41.87	14.57		
MSE	38.38	41.43	35.18	36.93	3.82		

On the other hand, with the larger cc-pVTZ basis set, CCSD(T) compares quite favorably to experiment in most cases (Table 6), except for pyridine and to a lesser extent cyclopentadiene. Due to the often unreliable error bars and inaccuracies associated with these historical experimental data[15,31], as well as possible remaining basis set limitations, we shall instead compare the various wavefunction-based methods relative to CCSD(T) for the remainder of this section. The mean and RMS errors for these magnetizability anisotropies relative to CCSD(T) are presented in Table 6. Additionally, the corresponding statistics for isotropic magnetizabilities are presented in Table 7.

Comparing the magnetizability anisotropies at the HF vs MP2 vs CCSD(T) levels shows that in 4 of the 6 cases, MP2 and OOMP2 overcorrect for correlation effects. These 4 cases (furan, thiophene, 1,3-dioxol-2-one, and cyclopentadiene) are therefore improved by regularization via κ-OOMP2. These 4 cases also shows strikingly small correlation at this level of basis. In the two remaining cases (benzene

Table 6: Calculated and experimental magnetizability anisotropies for various conjugated molecules. cc-pVTZ unless otherwise noted. Statistics calculated against CCSD(T) (10^{-30} JT^{-2})

Molecule	HF	MP2	OOMP2	κ-OOMP2	CCSD	CCSD(T)	exp.
benzene	-1125.54	-1069.91	-1056.94	-1081.22	-1047.36	-1027.63	-1036$\pm$40[81]
pyridine	-1077.14	-1029.05	-1003.57	-1032.58	-1011.74	-990.68	-953$\pm$12[82]
furan	-633.38	-681.06	-677.95	-669.79	-634.07	-639.10	-643$\pm$8[83]
thiophene	-841.75	-900.07	-899.71	-880.66	-837.80	-844.39	-832$\pm$18[83]
1,3-dioxol-2-one	-239.20	-248.32	-244.00	-244.33	-234.89	-237.40	-234$\pm$20[20]
cyclopentadiene	-553.19	-593.19	-598.75	-584.89	-547.30	-554.69	-570$\pm$5[20]
RMSE	53.40	40.25	35.54	36.16	12.67		
MSE	29.39	37.95	31.17	33.26	3.21		

and pyridine) MP2 and OOMP2 undercorrect relative to CCSD(T), with orbital optimization significantly improving upon the MP2 result. This undercorrection is quite significant. Regularization, which attenuates correlation effects associated with the smallest orbital gaps, therefore worsens the benzene and pyridine results. Interestingly, OOMP2 closely approaches CCSD for the benzene and pyridine cases, in contrast to overcorrelating for the other 4 cases.

Isotropic magnetizabilities show slightly different trends. Benzene and pyridine displays smaller correlation effects, around half that of the anisotropic magnetizabilities, whereas the other three molecules (furan, thiophene, 1,3-dioxol-2-one) shows slightly larger correlation effects. Cyclopentadiene shows strikingly small correlation, similar to the anisotropic case. Comparing the isotropic magnetizability at the HF vs MP2 vs CCSD(T) levels, instead of two distinct groups, we observe several distinct behaviours. For benzene and pyridine, MP2 again undercorrects relative to CCSD(T); orbital optimization via OOMP2 significantly improves upon the MP2 result, and even closely approaches CCSD(T). Regularization degrades the MP2 and OOMP2 results. For furan, MP2 overcorrects slightly relative to CCSD(T), while orbital optimization tempers the correlation contribution. For 1,3-dioxol-2-one, MP2 undercorrects relative

Table 7: Calculated isotropic magnetizability for various conjugated molecules evaluated in the cc-pVTZ basis (10^{-30} JT^{-2}). Error statistics are given relative to the CCSD(T) results.

Molecule	HF	MP2	κ-MP2	OOMP2	κ-OOMP2	CCSD	CCSD(T)
benzene	-999.36	-964.01	-972.68	-959.99	-971.39	-966.65	-954.09
pyridine	-880.70	-854.52	-862.74	-846.68	-859.40	-858.10	-845.74
furan	-747.79	-759.08	-757.69	-757.09	-756.52	-749.01	-756.54
thiophene	-993.86	-1004.85	-1000.94	-1001.93	-999.46	-987.78	-984.79
1,3-dioxol-2-one	-690.34	-685.18	-687.34	-680.15	-684.81	-682.78	-679.08
cyclopentadiene	-782.81	-794.88	-791.57	-793.97	-791.01	-783.26	-781.37
RMSE	24.36	11.58	13.35	9.03	11.74	8.10	
MSE	15.54	10.15	11.89	6.37	10.16	4.33	

to CCSD(T), while orbital optimization increases the correlation contribution. In these four molecules, OOMP2 performs surprisingly well relative to CCSD(T). Except for furan, regularization worsens the results for the other three molecules. In contrast, for thiophene, the MP2 correlation contribution has the wrong sign relative to CCSD(T); orbital optimization decreases the correlation contribution but retains the wrong sign.

Given the considerations mentioned above, it is clear that regularization of either the MP2 results for these conjugated species cannot give significant overall improvements since the two largest outliers are cases where correlation effects are underestimated with MP2 and OOMP2. Overall, the statistics suggest that MP2 moderately improves upon HF, reducing the RMSE for the magnetizability anisotropy by roughly 20%; and the isotropic magnetizability by roughly 50%. We also observe that all 4 MP2 methods give higher MSE than HF for anisotropy, similar to the results in Figure 1; whereas for the isotropic results, all 4 MP2 methods give lower MSE than HF, particularly OOMP2, which had more than half the MSE of HF's. Relative to MP2, there is a slight overall improvement with OOMP2 and an even smaller improvement with κ-OOMP2 (Table 6).

3.3 Evaluation of magnetizability exaltations in cyclic conjugated molecules

Other than energetic stabilization and geometric symmetry breaking, magnetizability exaltations have been suggested as a gauge for aromaticity and anti-aromaticity.[16–18] Qualitatively, with electron delocalization around a ring, the magnetizability perpendicular to the ring, and hence the isotropic magnetizability as well, should be enhanced relative to expected values due to the associated ring current. This exaltation provides a measure of aromaticity that is complementary to the susceptibility anisotropy discussed in the previous subsection. Of course, to define the exaltation of the magnetizability, it is also essential to have a reference. Traditionally, this reference is a theoretical molecule with the same bond structure but without conjugation. For example, benzene's reference would be the theoretical cyclo-hexatriene. Two conventions for calculating the magnetizability for these theoretical molecules have been employed. One is the Pascal system of atomic constants[84], and the other is the Haberditzl semiempirical increment system[85]. The Pascal and Haberditzl systems suffer from accuracy issues related to heteroatoms, small rings, non-cylindrical molecules, and charge[86]; missing constants or bond types also exclude novel systems from consideration, while the bond increment systems focuses on a single Lewis structure of the hypothetical non-aromatic ring system. Partly for these reasons, magnetizability exaltation has fallen out of favor as a criterion for aromaticity over the past 25 years. Indeed a recent review[87] commented that "due to the difficulty in quantifying aromaticity using this method and the need for an empirical reference, together with the development of computational methods that allow a more detailed and direct study of the magnetic properties, in a qualitative and quantitative fashion, this method is rarely used."

Modern alternative computational methods include those based on nucleus-independent chemical shifts[18] and those based on visualizing the current density.[88] While indeed these are valuable approaches, it is worth pointing out that magnetizability exaltations need not rely on empirical references. Here we will

define the out-of-plane magnetizability exaltation as the difference between the out-of-plane component of the magnetizability tensor (ξ_{zz}) of the aromatic molecule and that of a suitably chosen open chain analog with the same number of formal double bonds and lone pairs. Experimental comparison remains a possibility when susceptibility data for both ring and chain molecules is available. As a simple example, the open chain reference for benzene is hexatriene, $H_2C{=}CH{-}CH{=}CH{-}CH{=}CH_2$. Of course such references are typically not unique – even hexatriene has multiple conformations, though the all-trans form is a natural choice. Other molecules present more interesting alternative open chain references; for instance, we shall later examine N_2S_2 for which HNSNSH and H_2NSNS are both possible. The out-of-plane exaltation aims to single out the ring current effect by accounting for similar Lewis structures in both the aromatic rings and their open chain counterparts.

Aromatic, non-aromatic, and anti-aromatic molecules are expected to display large negative, around zero, and large positive exaltations respectively. Here we investigate small ring molecules with 2, 4, and 6 π electrons. All structures were optimized with ωB97M-V[89]/def2-TZVPDD.[90] In Table 8 we present out-of-plane magnetizability exaltations calculated with HF, MP2, κ-OOMP2, as well as CCSD and CCSD(T). Where different possible open chain references exist, our choice is specified (in some cases we will explore two alternative choices to assess the sensitivity of the exaltations to different reasonable choices of reference). Since our objective here is qualitative, the small cc-pVDZ basis was used for these calculations.

Starting with 6 π electrons, in addition to benzene, thiophene (C_4H_4S), cyclopentadiene anion ($C_5H_5^-$), and pyridine (C_5H_5N) all display the expected large negative magnetizability exaltations, associated with ring currents. In contrast, disulfur dinitride (N_2S_2) behaves as weakly anti-aromatic under the exaltation criteria, relative to the open-chain reference, HNSNSH. Interestingly, the results are virtually unchanged when using the alternative open-chain reference, H_2NSNS. It appears that the two straight

Table 8: Magnetizability exaltations for various molecules with 0, 2, or 6 π electrons calculated in the cc-pVDZ basis (10^{-30} J T^{-2}).

Molecule	Straight chain analog	HF	RI-MP2	κ-OOMP2	CCSD	CCSD(T)
		2 π electrons				
$C_2H_2N^+$	$H_2CC(H)NH$	-54.90	-69.94	-68.42	-65.75	-67.16
	H_2CNCH_2	-234.69	-228.11	-228.74	-221.42	-220.76
$C_3H_3^+$	$H_3CCCH_2^+$	-228.39	-221.02	-221.55	-221.07	-218.99
	$H_2CC(H)CH_2^+$	-47.89	-53.64	-53.10	-51.43	-52.24
CN_2H^+	$HNNCH_2$	-209.93	-205.27	-206.20	-200.96	-200.32
N_3^+		-213.45	-179.99	-189.82	-190.88	-188.09
		4 π electrons				
C_2H_2O	H_2COCH_2	-81.83	-37.54	-24.46	-42.24	-34.71
	$H_2CC(H)OH$	44.27	72.04	86.43	68.48	72.20
C_4H_4	s-trans	743.50	734.72	748.73	640.29	648.11
$C_5H_5^+$	s-cis	1209.29	1961.63	2027.48	1472.01	1598.06
	trans	1323.18	2100.45	2157.77	1596.96	1727.93
C_5H_6	trans 1,3 pentadiene	-175.40	-214.97	-207.72	-181.69	-186.87
	planar s-cis 1,3 pentadiene	-238.96	-296.12	-284.92	-256.29	-265.05
		6 π electrons				
S_2N_2	$SNSNH_2$	152.35	382.44	326.57	261.66	303.17
	HSNSNH	148.76	395.43	340.31	271.87	318.70
$C_5H_5^-$	cis	-718.63	-727.35	-729.51	-708.17	-704.59
	trans	-605.72	-606.83	-606.66	-592.97	-589.94
C_5H_5N	NCCCC	-521.11	-487.88	-491.27	-475.28	-456.70
	CCNCC	-511.46	-463.03	-468.09	-453.73	-432.74
C_6H_6	trans	-601.10	-546.79	-558.10	-534.88	-514.56

chain isomers display similar if not more delocalization than the N_2S_2 ring itself. In addition, calculated at the CCSD(T)/cc-pVTZ level, N_2S_2 has a magnetizability anisotropy of 67.0 10^{-30} JT^{-2}, which is much different from the normally large anisotropy that aromatic molecules possess. N_2S_2 has been previously characterized as weakly aromatic,[91,92] based on structural, energetic and chemical shift criteria. In simple terms, N_2S_2 is closer to 2-electron aromaticity than 6-electron aromaticity, because the two highest orbitals are essentially in and out of phase linear combinations of π-type lone pair orbitals on the two S atoms, giving bond order 1.25 for the N−S bonds. By contrast, other researchers had argued that N_2S_2 has diradicaloid character, for instance based on classical valence bond analysis[93]. On magnetizability grounds, N_2S_2 appears to continue to be an unconventional molecule.

Moving on to 4 π electron systems, cyclobutadiene, being the classic anti-aromatic molecule, displays a large positive exaltation as expected. Likewise, $C_5H_5^+$ also displays a very large positive exaltation. In contrast C_2H_2O, when considering the 70 kcal/mol more stable and electronically more similar $H_2CC(H)OH$ isomer, is predicted to be non-aromatic. For the group of molecules with 2 π electrons, all 4 molecules are predicted to be aromatic, with exaltations comparable to benzene and pyradine if normalized by π electron count.

We also consider cyclopentadiene C_5H_6, which was presented as an illustration against using out-of-plane magnetizability exaltation as an aromaticity criteria[94]. With our method, against both planar s-cis and trans isomers of 1,3-pentadiene, cyclopentadiene displays moderate negative exaltation, around 35 to 50% of benzene's. This suggests that not all of the exaltation results from the ring current effect, as the aforementioned authors stated[94]; nonetheless, given the difference in magnitude, out-of-plane magnetizability exaltation remains to appear to be a useful gauge of aromaticity.

Finally, it is interesting to briefly examine the effect of electron correlation on the magnetizability exaltations. Overall most of the studied molecules with strong magnetizability exaltations display small

correlation contributions, of most around 10%, with the striking exception of $C_5H_5^+$. For $C_5H_5^+$, MP2 and κ-OOMP2 provide relatively consistent exaltations, and the correlation contribution from both methods is around half of the exaltation from HF. The cause of this difference is in the magnetizability calculation of the ring molecule, where the χ_{zz} computed from CCSD(T) is more than twice that of HF. The exaltation calculated from CCSD(T) for $C_5H_5^+$ is qualitatively consistent with both RI-MP2 and κ-OOMP2.

4 Conclusions

In this work we have reported a new finite field implementation of magnetic properties, using gauge-including atomic orbitals, and applied it to the evaluation of magnetizabilities. This required development of software to implement the complex matrix elements, and to enable evaluation of energies using complex orbitals and amplitudes, as a consequence of the matrix elements. In return for overcoming those challenges, analytic derivatives are not required, and thus it is possible to assess the performance of new or uncommon electronic structure methods more readily.

As an illustration, we have reported tests of orbital optimized MP2 (OOMP2), and a recently proposed regularized OOMP2 method (κ-OOMP2) for magnetizabilities. These results for small molecules in the aug-cc-pVTZ basis show that κ-OOMP2 generally provides a significant improvement over MP2 itself, as well as over OOMP2, for magnetizabilities. However, it does not approach the accuracy of high-quality coupled cluster methods, such as CCSD(T). Results for isotropic magnetizabilities and magnetizability anisotropies for a set of 6 conjugated cyclic species in the smaller cc-pVTZ basis show smaller improvements with regularization for κ-OOMP2 over MP2, and no overall improvement relative to OOMP2.

Additionally we reexamined an old aromaticity criteria: the out-of-plane magnetizability exaltation.

Using a single straight chain molecule as reference instead of increment systems or empirical tables allows one to consider the difference in electronic structure and its underlying effects. We then applied this new regime on a set of aromatic and anti-aromatic molecules. These calculations proved interesting in several respects. First, while large negative exaltations are associated with aromaticity, we found one nominally aromatic species, N_2S_2, which displays a positive exaltation. This may rekindle debate about its aromaticity. Second, we found that errors in HF, MP2, and κ-OOMP2 magnetizability exaltations are significantly larger for anti-aromatic species, for the most part, consistent with the presence of stronger correlation effects.

In terms of future work, it will be interesting to see if significant improvements in the magnetizabilities predictions can be obtained by using orbitals from either κ-OOMP2 or density functional theory together with energy evaluation at the MP3 or scaled MP3 levels. Such models have been used with very promising results for relative energies.[49,95,96] and the effort to adapt an efficient MP3 code work with the complex orbitals and amplitudes associated with finite applied magnetic fields should be far less than implementing analytical second derivatives. Hopefully the framework built here will be helpful for exploring this and other unconventional possibilities for accurate and reasonably efficient evaluation of molecular magnetizabilities. We also intend to complete the extensions of our implementation necessary to evaluate chemical shifts, and in due course, scalar couplings.

Appendix A: GIAO Matrix Elements of the Diamagnetic Magnetizability

To arrive at a convenient expression for matrix elements of the diamagnetic magnetizability operator, Eq. 9, in the complex GIAO basis associated with a finite applied $\mathbf{B}$-field, we use the following shorthand notation for the overlap:

$$S_{\mu\nu}(l'+1) = \langle \omega_\mu | \omega_\nu(l'+1) \rangle \tag{17}$$

Here, l' is the polynomial power associated with the x-component of the Gaussian orbital that is a part of the GIAO ω_ν. Similarly, m' and n' are used for the y- and z-components, respectively. Hence, $S_{\mu\nu}(l'+1)$ is the overlap between GIAOs ω_μ and ω_ν with increased orbital angular momentum (x-component) of ω_ν. After some straightforward but cumbersome algebra we arrive at the following expression for matrix elements of the diamagnetic magnetizability operator given in Eq. 9:

$$\begin{aligned}
h_{\mu\nu}^{\mathrm{DM}} =& \frac{1}{8}\big[(B_y^2+B_z^2)\left(S_{\mu\nu}(l'+2)+2R_{\nu,x}S_{\mu\nu}(l'+1)+R_{\nu,x}^2S_{\mu\nu}\right) \\
&+(B_x^2+B_z^2)\left(S_{\mu\nu}(m'+2)+2R_{\nu,y}S_{\mu\nu}(m'+1)+R_{\nu,y}^2S_{\mu\nu}\right) \\
&+(B_x^2+B_y^2)\left(S_{\mu\nu}(n'+2)+2R_{\nu,z}S_{\mu\nu}(n'+1)+R_{\nu,z}^2S_{\mu\nu}\right) \\
&-2B_xB_y\left(S_{\mu\nu}(l'+1,m'+1)+R_{\nu,y}S_{\mu\nu}(l'+1)+R_{\nu,x}S_{\mu\nu}(m'+1)+R_{\nu,x}R_{\nu,y}S_{\mu\nu}\right) \\
&-2B_xB_z\left(S_{\mu\nu}(l'+1,n'+1)+R_{\nu,z}S_{\mu\nu}(l'+1)+R_{\nu,x}S_{\mu\nu}(n'+1)+R_{\nu,x}R_{\nu,z}S_{\mu\nu}\right) \\
&-2B_yB_z\left(S_{\mu\nu}(m'+1,n'+1)+R_{\nu,z}S_{\mu\nu}(m'+1)+R_{\nu,y}S_{\mu\nu}(n'+1)+R_{\nu,y}R_{\nu,z}S_{\mu\nu}\right)\big]
\end{aligned} \tag{18}$$

$R_{\nu,x}$, $R_{\nu,y}$ and $R_{\nu,z}$ denote the x, y and z-coordinates of the nucleus on which the GIAO ω_ν is centered.

Appendix B: GIAO Matrix Elements of the Paramagnetic Shielding

The matrix elements of the 3 spatial components of the paramagnetic shielding operator, Eq. 10 are given separately for clarity (though for instance the y component can be obtained as a cyclic permutation of the coordinates and the quantum numbers from the x component, and z can be obtained similarly from y).

$$\begin{aligned} h_{\mu\nu}^{\mathrm{PS},x} = -\frac{i}{2} B_x \big[& R_{\nu,z} \left(B_y S_{\mu\nu}(n'-1) + S_{\mu\nu}(m'+1, n'-1) \right) \\ & - 2\beta \left(B_y S_{\mu\nu}(n'+1) + S_{\mu\nu}(m'+1, n'+1) \right) \\ & - \frac{i}{2} \chi_{\nu,z} \left(B_y S_{\mu\nu} + S_{\mu\nu}(m'+1) \right) \\ & - \big[R_{\nu,y} \left(B_z S_{\mu\nu}(m'-1) + S_{\mu\nu}(m'-1, n'+1) \right) \\ & + 2\beta \left(B_z S_{\mu\nu}(m'+1) + S_{\mu\nu}(m'+1, n'+1) \right) \\ & + \frac{i}{2} \chi_{\nu,y} \left(B_z S_{\mu\nu} + S_{\mu\nu}(n'+1) \right) \big] \end{aligned} \tag{19}$$

$$\begin{aligned} h_{\mu\nu}^{\mathrm{PS},y} = -\frac{i}{2} B_y \big[& R_{\nu,x} \left(B_z S_{\mu\nu}(l'-1) + S_{\mu\nu}(l'-1, n'+1) \right) \\ & - 2\beta \left(B_z S_{\mu\nu}(l'+1) + S_{\mu\nu}(l'+1, n'+1) \right) \\ & - \frac{i}{2} \chi_{\nu,x} \left(B_z S_{\mu\nu} + S_{\mu\nu}(n'+1) \right) \\ & - \big[R_{\nu,z} \left(B_x S_{\mu\nu}(n'-1) + S_{\mu\nu}(l'+1, n'-1) \right) \\ & + 2\beta \left(B_x S_{\mu\nu}(n'+1) + S_{\mu\nu}(l'+1, n'+1) \right) \\ & + \frac{i}{2} \chi_{\nu,z} \left(B_x S_{\mu\nu} + S_{\mu\nu}(l'+1) \right) \big] \end{aligned} \tag{20}$$

$$
\begin{aligned}
h_{\mu\nu}^{\mathrm{PS},z} = -\frac{i}{2} B_z \big[& R_{\nu,y} \left(B_x S_{\mu\nu}(m'-1) + S_{\mu\nu}(l'+1, m'-1) \right) \\
& - 2\beta \left(B_x S_{\mu\nu}(m'+1) + S_{\mu\nu}(l'+1, m'+1) \right) \\
& - \frac{i}{2} \chi_{\nu,y} \left(B_x S_{\mu\nu} + S_{\mu\nu}(l'+1) \right) \\
& - \big[R_{\nu,x} \left(B_y S_{\mu\nu}(l'-1) + S_{\mu\nu}(l'-1, m'+1) \right) \\
& + 2\beta \left(B_y S_{\mu\nu}(l'+1) + S_{\mu\nu}(l'+1, m'+1) \right) \\
& + \frac{i}{2} \chi_{\nu,x} \left(B_y S_{\mu\nu} + S_{\mu\nu}(m'+1) \right) \big] \big]
\end{aligned}
\tag{21}
$$

In the above expressions, β is the gaussian exponent of the primitive GIAO ν and $\boldsymbol{\chi}_\nu$ is the vector

$$
\boldsymbol{\chi}_\nu = \mathbf{B} \times \mathbf{R}_\nu \tag{22}
$$

Acknowledgements

This work was supported by funding from the National Institutes of Health under Grant No. 5U01GM121667. TS gratefully acknowledges funding from the Deutsche Forschungsgemeinschaft (Grant Nos. STA 1526/1-1 and STA 1526/2-1).

References

[1] Davies, D. W. *Theory of the Electric and Magnetic Properties of Molecules*; John Wiley & Sons Ltd: Chichester, United Kingdom, 1967.

[2] Hinchliffe, A.; Munn, R. W. *Molecular Electromagnetism*; John Wiley & Sons Ltd, 1985.

[3] Sauer, S. P. A. *Molecular Electromagnetism: A Computational Chemistry Approach*; Oxford University Press: Oxford, United Kingdom, 2011.

[4] Ramsey, N. F. The Internal Diamagnetic Field Correction in Measurements of the Proton Magnetic Moment. *Phys. Rev.* **1950**, *77*, 567.

[5] Ramsey, N. F. Dependence of Magnetic Shielding of Nuclei upon Molecular Orientation. *Phys. Rev.* **1951**, *83*, 540–541.

[6] Ramsey, N. F. Magnetic Shielding of Nuclei in Molecules. *Phys. Rev.* **1951**, *78*, 699–703.

[7] Ramsey, N. F. Chemical Effects in Nuclear Magnetic Resonance and in Diamagnetic Susceptibility. *Phys. Rev.* **1952**, *86*, 243–246.

[8] Ramsey, N. F.; Purcell, E. M. Interactions between Nuclear Spins in Molecules. *Phys. Rev.* **1952**, *85*, 143–144.

[9] Ramsey, N. F. Pseudo-Quadrupole Effect for Nuclei in Molecules. *Phys. Rev.* **1953**, *89*, 527.

[10] Ramsey, N. F. Spin Interactions of Accelerated Nuclei in Molecules. *Phys. Rev.* **1953**, *90*, 232–233.

[11] Ramsey, N. F. Electron Coupled Interactions between Nuclear Spins in Molecules. *Phys. Rev.* **1953**, *91*, 303–307.

[12] Helgaker, T.; Jaszuński, M.; Ruud, K. Ab Initio Methods for the Calculation of NMR Shielding and Indirect Spin-Spin Coupling Constants. *Chem. Rev.* **1999**, *99*, 293–352.

[13] Helgaker, T.; Coriani, S.; Jørgensen, P.; Kristensen, K.; Olsen, J.; Ruud, K. Recent Advances in Wave Function-Based Methods of Molecular-Property Calculations. *Chem. Rev.* **2012**, *112*, 543–631.

[14] van Eldik, R.; Harvey, J. *Advances in Inorganic Chemistry. Theoretical and Computational Inorganic Chemistry*; Elsevier, 2010.

[15] Ruud, K.; Skaane, H.; Helgaker, T.; Bak, K. L.; Jørgensen, P. Magnetizability of Hydrocarbons. *J. Am. Chem. Soc.* **1994**, *116*, 10135–10140.

[16] Pauling, L. The Diamagnetic Anisotropy of Aromatic Molecules. *J. Chem. Phys.* **1936**, *4*, 673–677.

[17] von Ragué Schleyer, P.; Jiao, H. What is aromaticity? *Pure & Appl. Chem.* **1996**, *68*, 209–218.

[18] Jiao, H.; Von Ragué Schleyer, P.; Mo, Y.; McAllister, M. A.; Tidwell, T. T. Magnetic Evidence for the Aromaticity and Antiaromaticity of Charged Fluorenyl, Indenyl, and Cyclopentadienyl Systems. *J. Am. Chem. Soc.* **1997**, *119*, 7075–7083.

[19] Shoemaker, R. L.; Flygare, W. H. Molecular Quadrupole Moment, Molecular Magnetic Susceptibilities, and Molecular g Values in Benzene. *J. Chem. Phys.* **1969**, *51*, 2988–2991.

[20] Flygare, W. H.; Benson, R. C. The molecular Zeeman effect in diamagnetic molecules and the determination of molecular magnetic moments (g values), magnetic susceptibilities, and molecular quadrupole moments. *Mol. Phys.* **1971**, *20*, 225–250.

[21] Hyams, P. A.; Gerratt, J.; Cooper, D. L.; Raimondi, M. The calculation of molecular response properties using perturbed spin-coupled wave functions. II. Polarizability and magnetic susceptibility of H2 and LiH as functions of internuclear distance. *J. Chem. Phys.* **1994**, *100*, 4417–4431.

[22] Loibl, S.; Manby, F. R.; Schütz, M. Density fitted, local Hartree-Fock treatment of NMR chemical shifts using London atomic orbitals. *Mol. Phys.* **2010**, *108*, 477–485.

[23] Wilson, P. J.; Amos, R. D.; Handy, N. C. Density functional predictions for magnetizabilities and nuclear shielding constants. *Mol. Phys.* **1999**, *97*, 757–768.

[24] Tellgren, E. I.; Teale, A. M.; Furness, J. W.; Lange, K. K.; Ekström, U.; Helgaker, T. Non-perturbative calculation of molecular magnetic properties within current-density functional theory. *J. Chem. Phys.* **2014**, *140*, 034101.

[25] Reimann, S.; Borgoo, A.; Tellgren, E. I.; Teale, A. M.; Helgaker, T. Magnetic-Field Density-Functional Theory (BDFT): Lessons from the Adiabatic Connection. *J. Chem. Theory Comput.* **2017**, *13*, 4089–4100.

[26] Sauer, S. P. A.; Enevoldsen, T.; Oddershede, J. Paramagnetism of closed shell diatomic hydrides with six valence electrons. *J. Chem. Phys.* **1993**, *98*, 9748–9757.

[27] Cybulski, S. M.; Bishop, D. M. Calculation of magnetic properties. VI. Electron correlated nuclear shielding constants and magnetizabilities for thirteen small molecules. *J. Chem. Phys.* **1997**, *106*, 4082–4090.

[28] Cybulski, S. M.; Bishop, D. M. Calculation of magnetic properties VII. Electron-correlated magnetizability polarizabilities and nuclear shielding polarizabilities for nine small molecules. *Mol. Phys.* **1998**, *93*, 739–750.

[29] Gauss, J.; Ruud, K.; Kállay, M. Gauge-origin independent calculation of magnetizabilities and rotational g tensors at the coupled-cluster level. *J. Chem. Phys.* **2007**, *127*, 074101.

[30] Ruud, K.; Helgaker, T.; Bak, K. L.; Jørgensen, P.; Olsen, J. Accurate magnetizabilities of the isoelectronic series BeH-, BH, and CH+. The MCSCF-GIAO approach. *Chem. Phys.* **1995**, *195*, 157–169.

[31] Ruud, K.; Helgaker, T.; Jørgensen, P. The effect of correlation on molecular magnetizabilities and rotational g tensors. *J. Chem. Phys.* **1997**, *107*, 10599–10606.

[32] Cybulski, S. M.; Bishop, D. M. Electron-correlated calculations of magnetic properties: I. Magnetizability of H2 and HF. *Mol. Phys.* **1992**, *76*, 1289–1301.

[33] Cybulski, S. M.; Bishop, D. M. Calculations of magnetic properties. IV. Electron-correlated magnetizabilities and rotational g factors for nine small molecules. *J. Chem. Phys.* **1994**, *100*, 2019–2026.

[34] Loibl, S.; Schütz, M. Magnetizability and rotational g tensors for density fitted local second-order Møller-Plesset perturbation theory using gauge-including atomic orbitals. *J. Chem. Phys.* **2014**, *141*, 024108.

[35] Yoshizawa, T.; Hada, M. Relativistic and Electron-Correlation Effects on Magnetizabilities Investigated by the Douglas-Kroll-Hess Method and the Second-Order Moller-Plesset Perturbation Theory. *J. Comput. Chem.* **2009**, *30*, 2550–2566.

[36] Raghavachari, K.; Trucks, G. W.; Pople, J. A.; Head-Gordon, M. A fifth-order perturbation comparison of electron correlation theories. *Chem. Phys. Lett.* **1989**, *157*, 479–483.

[37] Lutnæs, O. B.; Teale, A. M.; Helgaker, T.; Tozer, D. J.; Ruud, K.; Gauss, J. Benchmarking density-functional-theory calculations of rotational g tensors and magnetizabilities using accurate coupled-cluster calculations. *J. Chem. Phys.* **2009**, *131*, 144104.

[38] Lehtola, S.; Dimitrova, M.; Fliegl, H.; Sundholm, D. Benchmarking Magnetizabilities with Recent Density Functionals. *J. Chem. Theory Comput.* **2021**, DOI: 10.1021/acs.jctc.0c01190.

[39] Lochan, R. C.; Head-Gordon, M. Orbital-optimized opposite-spin scaled second-order correlation: An economical method to improve the description of open-shell molecules. *J. Chem. Phys.* **2007**, *126*, 164101.

[40] Neese, F.; Schwabe, T.; Kossmann, S.; Schirmer, B.; Grimme, S. Assessment of Orbital-Optimized, Spin-Component Scaled Second-Order Many-Body Perturbation Theory for Thermochemistry and Kinetics. *J. Chem. Theory Comput.* **2009**, *5*, 3060–3073.

[41] Bozkaya, U.; Turney, J. M.; Yamaguchi, Y.; Schaefer, H. F.; Sherrill, C. D. Quadratically convergent algorithm for orbital optimization in the orbital-optimized coupled-cluster doubles method and in orbital-optimized second-order Møller-Plesset perturbation theory. *J. Chem. Phys.* **2011**, *135*, 104103.

[42] Bozkaya, U. Orbital-Optimized Second-Order Perturbation Theory with Density- Fitting and Cholesky Decomposition Approximations: An Efficient Implementation. *J. Chem. Theory Comput.* **2014**, *10*, 2371–2378.

[43] Stück, D.; Head-Gordon, M. Regularized orbital-optimized second-order perturbation theory. *J. Chem. Phys.* **2013**, *139*, 244109.

[44] Razban, R. M.; Stück, D.; Head-Gordon, M. Addressing first derivative discontinuities in orbital-optimised opposite-spin scaled second-order perturbation theory with regularisation. *Mol. Phys.* **2017**, *115*, 2102–2109.

[45] Lan, T. N.; Yanai, T. Correlated one-body potential from second-order Møller-Plesset perturbation theory: Alternative to orbital-optimized MP2 method. *J. Chem. Phys.* **2013**, *138*, 224108.

[46] Lee, J.; Head-Gordon, M. Regularized Orbital-Optimized Second-Order Møller-Plesset Perturbation Theory : A Reliable Fifth-Order Scaling Electron Correlation Model with Orbital Energy Dependent Regularizers. *J. Chem. Theory Comput.* **2018**, *14*, 5203–5219.

[47] Lee, J.; Head-Gordon, M. Distinguishing artificial and essential symmetry breaking in a single determinant: Approach and application to the C 60, C 36, and C 20 fullerenes. *Phys. Chem. Chem. Phys.* **2019**, *21*, 4763–4778.

[48] Lee, J.; Head-Gordon, M. Two single-reference approaches to singlet biradicaloid problems: Complex, restricted orbitals and approximate spin-projection combined with regularized orbital-optimized Møller-Plesset perturbation theory. *J. Chem. Phys.* **2019**, *150*, 244106.

[49] Bertels, L. W.; Lee, J.; Head-Gordon, M. Third-Order Møller-Plesset Perturbation Theory Made Useful? Choice of Orbitals and Scaling Greatly Improves Accuracy for Thermochemistry, Kinetics, and Intermolecular Interactions. *J. Phys. Chem. Lett.* **2019**, *10*, 4170–4176.

[50] Sen, S.; Tellgren, E. I. Benchmarking density functional approximations for diamagnetic and paramagnetic molecules in nonuniform magnetic fields. arXiv:2010/06042v1.

[51] London, F. Théorie Quantique des Courants Interatomiques Dans les Combinaisons Aromatiques. *J. Phys. Radium* **1937**, *8*, 397–409.

[52] Vaara, J. Theory and computation of nuclear magnetic resonance parameters. *Phys. Chem. Chem. Phys.* **2007**, *9*, 5399–5418.

[53] Fornberg, B. Generation of Finite Difference Formulas on Arbitrarily Spaced Grids. *Math. Comput.* **1988**, *51*, 699–706.

[54] Stopkowicz, S.; Gauss, J.; Lange, K. K.; Tellgren, E. I.; Helgaker, T. Coupled-cluster theory for atoms and molecules in strong magnetic fields. *J. Chem. Phys.* **2015**, *143*, 074110.

[55] Lehtola, S.; Dimitrova, M.; Sundholm, D. Fully numerical electronic structure calculations on diatomic molecules in weak and strong magnetic fields. *Mol. Phys.* **2019**, DOI: 10.1080/00268976.2019.1597989.

[56] Beer, M.; Kussmann, J.; Ochsenfeld, C. Nuclei-selected NMR shielding calculations: A sublinear-scaling quantum-chemical method. *J. Chem. Phys.* **2011**, *134*, 074102.

[57] Helgaker, T.; Jørgensen, P. An electronic Hamiltonian for origin independent calculations of magnetic properties. *J. Chem. Phys.* **1991**, *95*, 2595–2601.

[58] Irons, T. J. P.; Zemen, J.; Teale, A. M. Efficient Calculation of Molecular Integrals over London Atomic Orbitals. *J. Chem. Theory Comput.* **2017**, *13*, 3636–3649.

[59] Helgaker, T.; Jørgensen, P.; Olsen, J. *Molecular Electronic Structure Theory*; John Wiley & Sons Ltd: Chichester, 2000.

[60] Taketa, H.; Huzinaga, S.; O-ohata, K. Gaussian-Expansion Methods for Molecular Integrals. *J. Phys. Soc. Jpn* **1966**, *21*, 2313–2324.

[61] McMurchie, L. E.; Davidson, E. R. One- and Two-Electron Integrals over Cartesian Gaussain Functions. *J. Comput. Phys.* **1978**, *26*, 218–231.

[62] Dupuis, M.; Rys, J.; King, H. F. Evaluation of molecular integrals over Gaussian basis functions. *J. Chem. Phys.* **1976**, *65*, 111–116.

[63] King, H. F.; Dupuis, M. Numerical Integration Using Rys Polynomials. *J. Comput. Phys.* **1976**, *21*, 144–165.

[64] Gill, P. M. W.; Johnson, B. G.; Pople, J. A. Two-Electron Repulsion Integrals Over Gaussian. *Int. J. Quantum Chem.* **1991**, *40*, 745–752.

[65] Head-Gordon, M.; Pople, J. A. A method for two-electron Gaussian integral and integral derivative evaluation using recurrence relations. *J. Chem. Phys.* **1988**, *89*, 5777–5786.

[66] Pausch, A.; Klopper, W. Efficient evaluation of three-centre two-electron integrals over London orbitals. *Mol. Phys.* **2020**, *118*, e1736675.

[67] Handy, N. C.; Pople, J. A.; Head-Gordon, M.; Raghavachari, K.; Trucks, G. W. Size-Consistent Brueckner Theory Limited to Double Substitutions. *Chem. Phys. Lett.* **1989**, *164*, 185–192.

[68] Sherrill, C. D.; Krylov, A. I.; Byrd, E. F. C.; Head-Gordon, M. Energies and analytic gradients for a coupled-cluster doubles model using variational Brueckner orbitals: Application to symmetry breaking in O4+. *J. Chem. Phys.* **1998**, *109*, 4171–4181.

[69] Ortiz, J. V. Brueckner orbitals, Dyson orbitals, and correlation potentials. *Int. J. Quantum Chem.* **2004**, *100*, 1131–1135.

[70] Loibl, S.; Schütz, M. NMR shielding tensors for density fitted local second-order Moller-Plesset perturbation theory using gauge including atomic orbitals. *J. Chem. Phys.* **2012**, *137*, 084107.

[71] Shao, Y. et al. Advances in molecular quantum chemistry contained in the Q-Chem 4 program package. *Mol. Phys.* **2014**, *113*, 184–215.

[72] Epifanovsky, E.; Gilbert, A. T.; Feng, X.; Lee, J.; Mao, Y.; Mardirossian, N.; Pokhilko, P.; White, A. F.; Coons, M. P.; Dempwolff, A. L., et al. Software for the frontiers of quantum chemistry: An overview of developments in the Q-Chem 5 package. *J. Chem. Phys.* **2021**, *155*, 084801.

[73] Lee, J.; Bertels, L. W.; Small, D. W.; Head-Gordon, M. Kohn-sham density functional theory with complex, spin-restricted orbitals: Accessing a new class of densities without the symmetry dilemma. *Phys. Rev. Lett.* **2019**, *123*, 113001.

[74] Valatin, J. G. Generalized Hartree-Fock Method. *Phys. Rev.* **1961**, *122*, 1012–1020.

[75] Inc., W. R. Mathematica. `https://www.wolfram.com/mathematica`, Champaign, IL, 2021.

[76] Hô, M.; Hernándes-Pérez, J. M. Evaluation of Gaussian Molecular Integrals - I. Overlap Integrals. *Math. J.* **2012**, *14*, 1–14.

[77] Hô, M.; Hernándes-Pérez, J. M. Evaluation of Gaussian Molecular Integrals - II. Kinetic-Energy Integrals. *Math. J.* **2013**, *15*, 1–10.

[78] Hô, M.; Hernándes-Pérez, J. M. Evaluation of Gaussian Molecular Integrals - III. Nuclear-Electron Attraction Integrals. *Math. J.* **2014**, *16*, 1–13.

[79] Aidas, K. et al. The Dalton quantum chemistry program system. *WIREs Comput. Mol. Sci.* **2014**, *4*, 269–284.

[80] Stanton, J. F.; Gauss, J.; Cheng, L.; Harding, M. E.; Matthews, D. A.; Szalay, P. G. CFOUR, a quantum chemical program package. For the current version, see http://www.cfour.de.

[81] Lukins, P. B.; Buckingham, A. D.; Ritchie, G. L. D. Temperature dependence of the Cotton-Mouton effects of benzene, 1, 3, 5-trifluorobenzene, and hexafluorobenzene. *J. Phys. Chem.* **1984**, *88*, 2414–2418.

[82] Wang, J. H. S.; Flygare, W. H. Molecular g Values, Magnetic Susceptibility Anisotropies, Second Moments of the Electronic Charge Distribution, and Molecular Quadrupole Moments in Pyridine. *J. Chem. Phys.* **1970**, *52*, 5636–5640.

[83] Sutter, D. H.; Flygare, W. H. Molecular g values, magnetic susceptibility anisotropies, second moment of the charge distribution, and molecular quadrupole moments in furan and thiophene. *J. Am. Chem. Soc.* **1969**, *91*, 4063–4068.

[84] Pascal, P. Magnetochemical researches. *Ann. Chim. Phys.* **1910**, *19*, 5.

[85] Haberditzl, W. Advances in molecular diamagnetism. *Angew. Chem. Int. Ed.* **1966**, *5*, 288.

[86] Dauben, H. J.; Wilson, J. D.; Laity, J. L. Diamagnetic susceptibility exaltation as a criterion of aromaticity. *J. Am. Chem. Soc.* **1968**, *90*, 811–813.

[87] Gershoni-Poranne, R.; Stanger, A. Magnetic criteria of aromaticity. *Chem. Soc. Rev.* **2015**, *44*, 6597–6615.

[88] Guo, R.; Uddin, M. N.; Price, L. S.; Price, S. L. Calculation of Diamagnetic Susceptibility Tensors of Organic Crystals: From Coronene to Pharmaceutical Polymorphs. *J. Phys. Chem. A* **2020**, *124*, 1409–1420, PMID: 31951408.

[89] Mardirossian, N.; Head-Gordon, M. ωB97M-V: A combinatorially optimized, range-separated hybrid, meta-GGA density functional with VV10 nonlocal correlation. *J. Chem. Phys.* **2016**, *144*, 214110.

[90] Weigend, F.; Häser, M.; Patzelt, H.; Ahlrichs, R. RI-MP2: Optimized auxiliary basis sets and demonstration of efficiency. *Chem. Phys. Lett.* **1998**, *294*, 143–152.

[91] Jung, Y.; Heine, T.; Schleyer, P.; Head-Gordon, M. Aromaticity of four-membered-ring 6 pi-electron systems: N2S2 and Li2C4H4. *J. Am. Chem. Soc.* **2004**, *126*, 3132–3138.

[92] Karadakov, P. B.; Al-Yassiri, M. A. H.; Cooper, D. L. Magnetic Shielding, Aromaticity, Antiaromaticity and Bonding in the Low-Lying Electronic States of S2N2. *Chem. Eur. J.* **2018**, *24*, 16791–16803.

[93] Braïda, B.; Derat, E.; Humbel, S.; Hiberty, P. C.; Shaik, S. The Valence Bond Workshop in Paris: The Phoenix Rises from the Ashes or, Has a Love Story with MO-Based Theories Begun? *ChemPhysChem* **2012**, *13*, 4029–4030.

[94] Fleischer, U.; W. Kutzelnigg, W.; P. Lazzeretti, P.; Muehlenkamp, V. IGLO Study of Benzene and Some of Its Isomers and Related Molecules. Search for Evidence of the Ring Current Model. *J. Am. Chem. Soc.* **1994**, *116*, 5298–5306.

[95] Rettig, A.; Hait, D.; Bertels, L. W.; Head-Gordon, M. Third-Order Møller–Plesset Theory Made More Useful? The Role of Density Functional Theory Orbitals. *J. Chem. Theory Comput.* **2020**, *16*, 7473–7489.

[96] Loipersberger, M.; Bertels, L. W.; Lee, J.; Head-Gordon, M. Exploring the Limits of Second-and Third-Order Møller–Plesset Perturbation Theories for Noncovalent Interactions: Revisiting MP2. 5 and Assessing the Importance of Regularization and Reference Orbitals. *J. Chem. Theory Comput.* **2021**, *17*, 5582–5599.